TIPE2 inhibits GC via regulation of cell proliferation, apoptosis and inflammation

ZHENHE LIN[1,2], WENMING LIU[1], CHUANXING XIAO[1], YANYUN FAN[1],
GUOHONG ZHUANG[2] and ZHONGQUAN QI[2]

[1]Department of Gastroenterology, Zhongshan Hospital Affiliated to Xiamen University, Xiamen, Fujian 361004;
[2]Organ Transplantation Institute, Anti-Cancer Research Center, Medical College of Xiamen University,
Xiamen, Fujian 361102, P.R. China

Abstract. Gastric cancer (GC), a type of gastric mucosal epithelium disease caused by common malignant tumors, has become a major threat to human health and survival. Tumor necrosis factor-α-induced protein-8 like-2 (TIPE2) is a negative immune regulatory factor that is selectively expressed in immune organs, immune cells and various epithelial cells and serves an important role in the maintenance of human physiological immune homeostasis. In our preliminary study, we found that the expression of TIPE2 was downregulated or absent in GC tissues compared with normal gastric mucosa tissues, indicating that TIPE2 may play a significant role in the development of GC. To clarify the role of TIPE2 in the progression of human GC and to elucidate the underlying mechanism, the association between TIPE2 and phosphatidylinositol 3-kinase (PI3K)/AKT, the cell cycle, the caspase-related apoptosis pathway and the NF-κB signaling pathway were investigated through western blot and flow cytometric analysis. It was determined that TIPE2 inhibited GC cell proliferation mainly by reducing the expression of phosphorylated AKT and ERK, which caused subsequent inhibition of the PI3K-AKT and Ras-Raf-MEK-ERK1/2 signaling pathways. Additionally, we investigated the relationship between TIPE2 and GC and discovered that TIPE2 inhibited tumor progression via growth, apoptosis and inflammatory pathways. The results of the present study provided a theoretical basis for the development and application of TIPE2 as an antitumor agent.

Introduction

Gastric cancer (GC) is one of the most common malignancies and the second leading cause of cancer-related deaths worldwide. It accounted for ~723,000 cancer-associated deaths (~10% of the total recorded deaths from cancer) in 2012 worlwide (1). In underdeveloped regions of Asia, Eastern Europe and South America, there is a high incidence of GC. In China, the morbidity and mortality of GC is increasing with population size, prompting an urgent need to develop more effective treatments and identify novel therapeutic targets for GC (2,3). Although the pathogenesis of GC is not fully understood, it is thought that immunomodulatory disorders, such as persistent inflammation, play a significant role in its promotion (4). Anti-inflammatory molecules may therefore, be potential candidates for cancer treatment.

TNFAIP8-like 2 (TIPE2) is a member of the tumor necrosis factor-a inducible protein-8 (TNFAIP8) family. Recent studies have revealed that TIPE2 is a negative immune regulator that is selectively expressed in immune organs and cells, and serves an important role in the maintenance of human physiological and immunological homeostasis (5). TIPE2 knockout in mice induced inflammation in multiple organs. TIPE2 was found to execute its negative regulatory role by binding to caspase-8 and thus, inhibiting activating protein-1 and nuclear factor-κB (NF-κB) stimulation in macrophages (5,6).

TIPE2 has been reported to be a negative regulator of the human immune response, as demonstrated by its downregulation in peripheral blood mononuclear cells (PBMCs) obtained from patients with systemic lupus erythematosus (7) and chronic hepatitis B (8). In addition to its role as a negative

Correspondence to: Professor Guohong Zhuang or Professor Zhongquan Qi, Organ Transplantation Institute, Anti-Cancer Research Center, Medical College of Xiamen University, Xiamen, Fujian 361102, P.R. China
E-mail: zhgh@xmu.edu.cn
E-mail: zqqi@xmu.edu.cn

regulator of the immune response, TIPE2 is expressed in various epithelial cell types, including esophageal and cervical squamous epithelial cells, transitional epithelial cells of the bladder and ureter, and glandular epithelial cells of the stomach, colon and appendix (9,10), thus indicating an activity beyond immune cell regulation.

It has been reported that TIPE2 levels are reduced in hepatocellular cancer (HCC) cells (11), and TIPE2 overexpression decreased tumor growth and metastasis in a xenograft mouse model bearing a human HCC cell line. Sun *et al* (11) reported that the expression of TIPE2 was either completely suppressed or significantly decreased in human liver cancer. Zhu *et al* found that adenovirus-directed expression of TIPE2 suppressed GC growth via induction of apoptosis and inhibition of AKT and ERK1/2 signaling in AGS and HGC-27 GC cells (12). In addition, TIPE2 promoted a p27-associated signaling cascade that decreased GC cell proliferation (13). A biochemical characterization study of TIPE2, conducted by Cao *et al*, revealed that TIPE2 binds to RAC1 to reduce its activity and inhibit the activation of MMP9 and Upa, thereby suppressing metastasis (14). In contrast, Li *et al* reported that TIPE2 was overexpressed in colon cancer tissues (15), suggesting that the function of TIPE2 may vary depending on the type of cancer cells.

The function of TIPE2 in GC remains unclear. In the present study, we aimed to identify the role of TIPE2 in GC cell migration and proliferation. To characterize the functional consequence of TIPE2 downregulation in GC cells, we generated a TIPE2-silenced gastric cell line.

As gastric carcinoma has been reported to be related with epithelial inflammation, we used LPS to stimulate GC cells and mimic the inflammatory process observed during tumorigenesis. In TIPE2-silenced GC cell lines, cell death was reduced following stimulation with LPS, but not in unstimulated cells. In the present study, a model for the role of TIPE2 in GC development is presented and discussed. We aimed to explain how TIPE2 inhibited tumor growth via proliferation, apoptosis and inflammatory pathways.

Materials and methods

Patients. For RNA detection, 42 tumor samples were collected from GC patients at the Zhongshan Hospital of Xiamen University between January 2014 and January 2015. This cohort was comprised of 7 females and 35 males, ranging from 43 to 88 years old. For immunohistochemistry detection, 63 tumor samples were collected from GC patients at the Zhongshan Hospital of Xiamen University between January 2013 and January 2015. Written informed consent for the study was provided by all participants. The study was approved by the Medical Ethics Committee of Zhongshan Hospital of Xiamen University.

Cell culture. Human BGC823 and SGC7901 GC cells were purchased from the Chinese Academy of Medical Sciences (Shanghai, China). BGC823 cells were maintained in RPMI-1640 medium (Gibco; Thermo Fisher Scientific, Inc., Waltham, MA, USA) supplemented with 10% fetal bovine serum (FBS; HyClone Laboratories; GE Healthcare Life Sciences, Logan, UT, USA), 100 U/ml penicillin and 100 U/ml streptomycin in a humidified atmosphere with 5% CO_2 at 37˚C.

Establishment of a TIPE2-overexpressing GC cell line. The TIPE2-overexpression plasmid was constructed by cloning human TIPE2 cDNA into a GV218 lentivirus vector. Briefly, total cellular RNA was purified using an RNA extraction kit (Tiangen Biotech Co., Ltd., Beijing, China) and the full-length coding sequence (CDS) of TIPE2 was amplified via reverse transcription-PCR (RT-PCR). The first-strand cDNA was synthesized using a Reverse Transcription kit (Tiangen Biotech Co.,Ltd. PCR was performed using cDNA as a template with the following TIPE2-specific primer pair: TIPE2-AgeI-F, 5'-GAG GATCCCCGGGTACCGGTCGCCACCATGGAGTCCTTC AGCTC-3' and TIPE2-Age I-R, 5'-TCACCATGGTGGCGA CCGGGCTCAGAGCTTCCCTTC-3'. The fragments were sub-cloned into a GV218 lentivirus vector and verified by DNA sequencing. Pack virus according to Lenti-Easy Packaging system (Shanghai GeneChem, Co., Ltd., Shanghai, China). BGC823 and SGC7901 cells were transfected and selected with 2 μg/ml puromycin. Separated cell clones were confirmed via western blot analysis and stored for further experiments.

Cell viability assay. Cell viability was evaluated using a CCK-8 kit (Beyotime Institute of Biotechnology, Haimen, China) according to the manufacturer's instructions. Briefly, cells were seeded into 96-well plates at $1x10^4$ cells/well. After culturing for the indicated time periods, CCK-8 solution was added to each well and incubated for 1 h. We determined the absorbance for each well at a wavelength of 450 nm using a microplate reader (Bio-Tek Instruments, Inc., Winooski, VT, USA). Experiments for each time-point were performed in quadruplicate and three times independently.

Scratch assay. Cell migration was evaluated using a scratch assay. Briefly, we marked the bottom of each 6-well plate with a horizontal line as a reference point for image acquisition. BGC823 cells were seeded into 6-well plates and cultured to 90% confluence. Cells were scratched using a 10-μl pipette tip to create a cell-free area and washed gently with PBS three times to remove detached cells. Plates were then incubated for 48 h in Dulbecco's modified Eagle medium (DMEM; HyClone Laboratories; GE Healthcare Life Sciences) containing 4% FBS. Cell-free areas were imaged, and the gap distance was quantitatively calculated using ImageJ 1.46r software (National Institutes of Health, Bethesda, MD, USA).

Real-time reverse transcription-polymerase chain reaction (RT-PCR). Total cellular RNA was extracted using an RNA Extraction kit (Tiangen Biotech Co., Ltd.). First-strand cDNA was synthesized using a Reverse Transcription kit (Tiangen Biotech Co., Ltd.) and subjected to real-time PCR analysis. PCR was performed in triplicate with an ABI Step One Plus Real-Time PCR (Applied Biosystems; Thermo Fisher Scientific, Inc.) under the following conditions: 95˚C for 2 min followed by 40 cycles at 95˚C for 10 sec, 60˚C for 30 sec and 72˚C for 30 sec, with a final extension at 72˚C for 10 min as previously described (16,17). Sequences of the gene-specific primers (sense and antisense, respectively) were: 5'-TCTTCC AGCCTTCCTTCCT-3' and 5'-AGCACTGTGTTGGCGTAC AG-3' for β-actin; and 5'-CACCGCAATGGCTCCTTT-3' and 5'-CACCAACTCTAGCAGCACATC-3' for TIPE2.

Western blot analysis. Cells were harvested and lysed in RIPA buffer [1% Triton, 0.1% SDS, 0.5% deoxycholate, 1 mM EDTA, 20 mM Tris (pH 7.4), 150 mM NaCl, 10 mM NaF, 1 mM Na_3VO_4, and 0.1 mM phenylmethyl sulfonyl fluoride] on ice for 30 min. We collected the supernatants via centrifugation and detected the concentrations of proteins using a BCA Assay kit (Pierce; Thermo Fisher Scientific, Inc.). Equal amounts of the prepared protein were separated by 10% SDS-PAGE and transferred onto polyvinylidene fluoride (PVDF) (Millipore, Billerica, MA, USA) membranes. The PVDF membranes were blocked in 5% non-fat milk in TBST at room temperature for 1 h, and then incubated overnight at 4°C with primary antibodies against the following proteins: TIPE2 (1:1,000; rabbit ployclonal; cat. no. 15940-1-AP; ProteinTech, Group, Inc., Chicago, IL, USA), β-actin (1:1,000; mouse monoclonal; cat. no. sc-58673; Santa Cruz Biotechnology, Inc., Dallas, TX, USA), AKT (1:1,000; mouse monoclonal; cat. no. sc-377457; Santa Cruz Biotechnology), p-AKT (1:1,000; mouse monoclonal; cat. no. sc-52940; Santa Cruz Biotechnology), CDK1 (1:1,000; mouse monoclonal; cat. no. 9116), p-CDK1 (1:1,000; rabbit monoclonal; cat. no. 4539), cyclin B1 (1:2,000; rabbit polyclonal; cat. no. 4138), Bcl-2 (1:1,000; mouse monoclonal; cat. no. 15071), cleaved caspase-3 (1:1,000; rabbit ployclonal; cat. no. 9661), cleaved caspase-9 (1:1,000; rabbit monoclonal; cat. no. 20750), IκBα (1:1,000; rabbit monoclonal; cat. no. 4812), p-IKK (1:1,000; rabbit monoclonal; cat. no. 2697), p-p65 (1:1,000; rabbit monoclonal; cat. no. 3033), vimentin (1:1,000; rabbit monoclonal; cat. no. 5741), N-cadherin (1:1,000; rabbit monoclonal; cat. no. 13116), E-cadherin (1:1,000; mouse monoclonal; cat. no. 14472; all were from Cell Signaling Technology, Inc., Beverly, MA, USA). The membranes were washed three times with TBST, and then were incubated with an HRP-conjugated secondary antibody (1:10,000; goat ployclonal; cat. no. LP31460; Xiamen Lulong Biotech Co., Ltd., Xiamen, China) for 1 h at 37°C. Immunoreactive products were visualized using an enhanced chemiluminescence system (GE Healthcare Life Sciences, Little Chalfont, UK).

Immunohistochemistry (IHC). Paraffin-embedded tissue sections were deparaffinized with xylene and gradually rehydrated. Each section was added to a solution of 0.3% hydrogen peroxide and 10% methanol for 10 min at room temperature to block the activity of endogenous peroxidase. Goat serum (Invitrogen; Thermo Fisher Scientific, Inc.) was used to block non-specific staining. Sections were incubated with an anti-TIPE2 antibody (1:1,000; mouse ployclonal; cat. no. H00079626-B01P; Abnova, Taipei, Taiwan) overnight at 4°C. After washing with PBS, secondary staining was performed with an HRP-conjugated secondary antibody (1:10,000; goat ployclonal; cat. no. LP31460; Xiamen Lulong Biotech Co., Ltd.). Immunoreactivity was detected using a freshly prepared DAB solution (Fuzhou Maixin Biotech. Co., Ltd., Fuzhou, China), followed by counterstaining with hematoxylin and dehydration in graded concentrations of alcohol and dimethyl benzene. The sections were observed using optical microscopy (Olympus BX51; Olympus Corp., Tokyo, Japan).

Flow cytometric analysis. The effects of TIPE2 on the cell cycle were detected via flow cytometric analysis. Briefly, cells were trypsinized with EDTA-free trypsin and centrifuged to obtain a cell pellet, following which the supernatant was discarded and the cells were washed with ice-cold PBS. Cells were re-suspended and fixed in 70% pre-cooled ethanol at 4°C overnight. Ethanol-fixed cells were centrifuged, the supernatant was discarded, and the cells were washed three times with PBS to remove residual ethanol. Cells were re-suspended in 1 ml staining solution [50 μg/ml propidium iodide (PI)] containing 10 μg/ml RNase A and stained for 15 min at room temperature. Stained cells were analyzed by flow cytometry (BD Biosciences, Franklin Lakes, NJ, USA). Cell cycle distribution was analyzed using ModFit v.3.0 software (Verity Software House, Topsham, ME, USA). The effect of TIPE2 on cell apoptosis was determined by flow cytometry using an FITC-Annexin V Apoptosis Detection kit (BD Biosciences). Briefly, ~1×10^5 cells were resuspended in 100 μl binding buffer, to which 5 μl FITC-Annexin V and 10 μl PI were added. Cells were gently vortexed followed by incubation for 15 min at room temperature, in the dark. Finally, we added 400 μl binding buffer to each tube and analyzed the solutions via flow cytometry within 1 h.

Detection of caspase activity. The activity of caspase-3, caspase-8 and caspase-9 was analyzed using Caspase-Glo®3/7 Assay System, Caspase-Glo®8 Assay System and Caspase-Glo®9 Assay System (Promega, Madison, WI, USA) according to the manufacturer's instructions. Briefly, 96-well plates containing cells were removed from the incubator and the plates were allowed to equilibrate to room temperature. Caspase-Glo® reagent (100 μl) was added to each well of a white-walled 96-well plate containing 100 μl of blank or cells in culture medium. The contents of the wells were gently mixed and incubated at room temperature for 30 min. Finally, the luminescence of each sample was assessed on a plate-reading luminometer (PerkinElmer EnVision; PerkinElmer, Waltham, MA, USA) as directed by the manufacturer's instructions.

ELISA. Levels of the inflammatory cytokines IL-1β (cat. no. BRK0181; BioRike, Changsha, China), IL-6 (cat. no. BRK0049; BioRike) and TNF-α (cat. no. BRK0122; BioRike) were detected using an ELISA assay. After treatment with LPS (20 ng/ml) for 24 h, the supernatants were collected and the IL-1β, IL-6 and TNF-α standard protein samples were added to the wells, which were then sealed and incubated at room temperature for 1 h. Following incubation, the wells were washed 4 times with a buffer, following which a biotin-conjugated detection antibody was added to each well and incubated for 1 h at room temperature. The wells were subsequently washed another 4 times, before streptavidin-conjugated HRP was added and incubated for 30 min. Finally, the wells were washed 4 times, and the chromogenic substrate TMB was added to develop the color. The absorbance was read at 405 nm.

Promoter reporters and dual-luciferase assays. SGC7901/vector and SGC7901/TIPE2 cells were transfected with pGL4-NF-κB-Luc (Promega) and pRL-TK-vector (Promega) using the Lipofectin reagent (Life Technologies, Inc., Gaithersburg, MD, USA). After 24 h of transfection, cells were treated with or without LPS (10 ng/ml) for 12 h. The cells
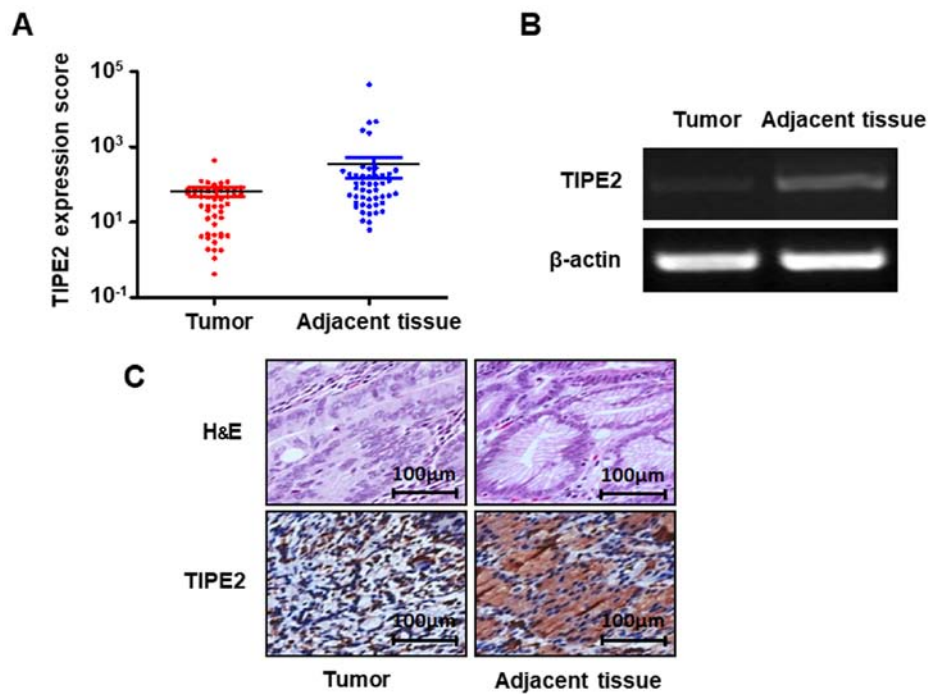
Figure 1. Expression of TIPE2 in GC and normal gastric mucosa. (A and B) Total mRNA was extracted from the tumor and adjacent tissues, and the expression of TIPE2 mRNA was detected by RT-PCR and (C) immunohistochemistry. RT-PCR, real-time reverse transcription-polymerase chain reaction.

Table I. TIPE2 protein expression in GC and adjacent tissues.

Clinical data	Negative (-)	Weakly positive (+)	Positive (++)	Strongly positive (+++)	P-value
Normal gastric mucosa	0	19	42	2	<0.05
GC	4	49	9	1	

GC, gastric cancer.

were then harvested in passive lysis buffer (Promega). Firefly luciferase and *Renilla* luciferase activities were quantified using the Dual-Luciferase Assay System (Promega). Changes in firefly luciferase activity were calculated relative to the *Renilla* luciferase.

Statistical analysis. Experimental data are presented as the mean ± standard deviation (SD). Differential expression of the TIPE2 protein between the GC and adjacent non-cancerous tissues was analyzed using the Chi-square test. The Student's t-test was used to compare differences between groups, which were then analyzed using SPSS v.11.0 software (SPSS, Inc., Chicago, IL, USA). A value of $P<0.05$ was considered to indicate a statistically significant difference.

Results

Expression of TIPE2 in gastric carcinoma and normal gastric mucosa. The TIPE2 protein was first discovered in 2008 by Sun *et al* (University of Pennsylvania) in the neurological tissues of patients with experimental autoimmune encephalomyelitis. The protein was revealed to play an important

regulatory role in human immune homeostasis (5). To detect differences in TIPE2 expression between GC and adjacent normal gastric mucosae, we collected paired tissue samples from 42 patients with GC who were admitted to Zhongshan Hospital of Xiamen University between January 2014 and January 2015. Total RNA was extracted and the expression of TIPE2 mRNA was detected by RT-PCR in gastric carcinoma and normal gastric mucosa tissues. As shown in Fig. 1A and B, the mRNA expression of TIPE2 was significantly lower in GC tissues than in normal gastric mucosa ($P<0.05$).

In order to assess the relationship between TIPE2 expression and GC tissues, we used immunohistochemistry to detect the expression of TIPE2 in tumor tissue samples collected from 63 patients with GC at the Zhongshan Hospital of Xiamen University from January 2013 to January 2015. The results showed that TIPE2 staining ranged from light-brown to brown in the normal gastric mucosae, while TIPE2 staining was negative or relatively weak in GC cells. Further analysis of the 63 tissue pairs revealed that TIPE2 was expressed in 69.84% (44/63) of the adjacent tissues, which was significantly higher than the 15.87% (10/63) of GC tissues ($P<0.05$) (Fig. 1C; Table I). These results indicated that TIPE2
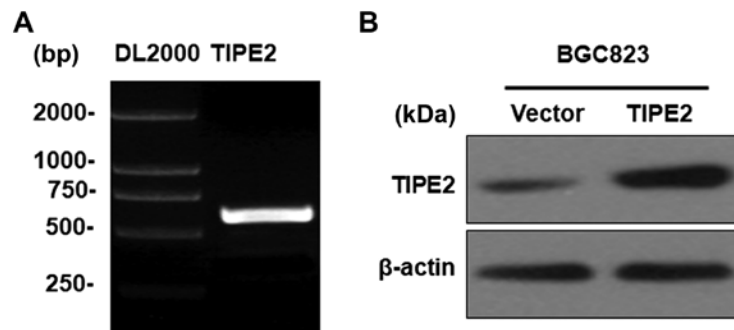
Figure 2. Establishment of a TIPE2-overexpressing stable cell line. (A) Human TIPE2 CDS was cloned by RT-PCR. (B) Western blot analysis of lenti-viral-mediated TIPE2 expression. CDS, code domain sequence; RT-PCR, reverse transcription-polymerase chain reaction.

expression was reduced in GC, and that TIPE2 has a central role in the development and progression of GC.

Establishment of a stable TIPE2-overexpressing cell line. In order to explore the function and mechanism of TIPE2 in GC, the fragment containing a 555-bp CDS of human TIPE2 was successfully cloned (Fig. 2A). The fragment was subcloned into the GV218 lentiviral vector and verified by DNA sequencing (data not shown). The vectors were transfected into the BGC823 GC cell line to generate a TIPE2-overexpressing stable cell line, named BGC823/TIPE2, and a control cell line, named BGC823/Vector. TIPE2 overexpression was detected via western blotting (Fig. 2B).

TIPE2 inhibits GC cell proliferation. To explore the effect of TIPE2 on GC cell growth, the viability of BGC823/Vector and BGC823/TIPE2 cells were assessed at different time-points (days 1-5) using a CCK-8 assay. Compared with the vector control group, TIPE2 significantly suppressed BGC-823 tumor cell growth *in vitro* on day 3, days 4 and 5 after transfection in a time-dependent manner (P<0.05; Fig. 3A). Furthermore, *in vivo* EdU-incorporation assays revealed that TIPE2 caused a marked reduction in the proportion of BGC-823 human GC cells that incorporated EdU (P<0.05; Fig. 3B and C). Collectively, these results indicated that TIPE2 increased DNA synthesis and inhibited the proliferation of GC cells.

TIPE2 causes G_2/M phase cell-cycle arrest in GC cells. To determine whether TIPE2 inhibited cell-cycle progression in GC cells, BGC823/Vector and BGC823/TIPE2 cells were cultured without serum for 12 h and then cultured in normal medium. The cell cycle distribution was analyzed by flow cytometry after 24 h. The results revealed that the percentage of cells in the S phase decreased from 33.16 to 27.36% and that the cells of the G_2/M phase increased from 8.53 to 15.23%, following TIPE2 overexpression in BGC823 cells compared with the control group (Fig. 4A). These results indicated that TIPE2 affected the cell cycle distribution in GC cells and could block the cell cycle in the G_2/M phase.

In order to further study the specific molecular mechanism of TIPE2-induced G_2/M phase arrest, we detected the expression of AKT, p-AKT, ERK, p-ERK, CDK1, p-CDK1 and cyclin B1 in GC cells after TIPE2 overexpression using western blotting. The results revealed that TIPE2 overexpression could downregulate the expression of p-AKT, p-ERK,

CDK1 and cyclin B1 in GC cells and upregulate the expression of p-CDK1 protein (Fig. 4B-E). These results indicated that TIPE2-induced G_2/M phase cell cycle arrest was associated with the inhibition of p-AKT, p-ERK, CDK1 and cyclin B1, as well as the promotion of p-CDK1 in the GC cell cycle.

TIPE2 inhibits the migration of GC cells. Tumor metastasis is an important hallmark of cancer, resulting in ≤90% of cancer-associated deaths (1). To investigate the effect of TIPE2 on GC migration *in vitro*, a scratch-wound assay was performed using BGC-823/Vector and BGC-823/TIPE2 cells. As displayed in Fig. 5A and B, TIPE2 overexpression evidently inhibited the migration of BGC823 GC cells compared with the control (P<0.05). Our data indicated that TIPE2 negatively regulated GC cell motility.

Epithelial-mesenchymal transition (EMT) is an important process by which a malignant tumor can obtain metastatic ability (18,19). The mechanism by which TIPE2 inhibited tumor migration was determined by assessing the expression changes in EMT-related factors. Western blot analysis revealed that the expression of E-cadherin in the TIPE2-overexpressing group was significantly upregulated compared with the control group, while the expression of N-cadherin and vimentin was inhibited, indicating that the effect of TIPE2 on cell migration may occur via the regulation of the expression of EMT-related factors in GC (Fig. 5C and D).

TIPE2 promotes GC cell apoptosis. The growth of cancer cells is affected by two major factors, namely proliferation and apoptosis. The aforementioned results indicated that TIPE2 inhibited BGC823 cell proliferation. However, whether TIPE2 has a potential role on the apoptosis of GC cells remained under question. Therefore, a TIPE2-overexpressing vector was constructed and transiently transfected into the BGC823 GC cell line over 48 h. Following this, we conducted flow cytometry to determine the effect of TIPE2 on BGC823 cell apoptosis. The results revealed that the ratio of BGC823cells in early-stage and late-stage apoptosis increased from 14.2 to 22.1% after TIPE2 overexpression (Fig. 6A). These results indicated that TIPE2 could effectively promote the apoptosis of BGC823 cells *in vitro*.

To elucidate the molecular mechanism responsible for TIPE2-mediated apoptosis, the expression levels of apoptosis-related proteins such as Bcl-2, caspase-9, caspase-3 and PARP in TIPE2-transfected and vector-transfected BGC823
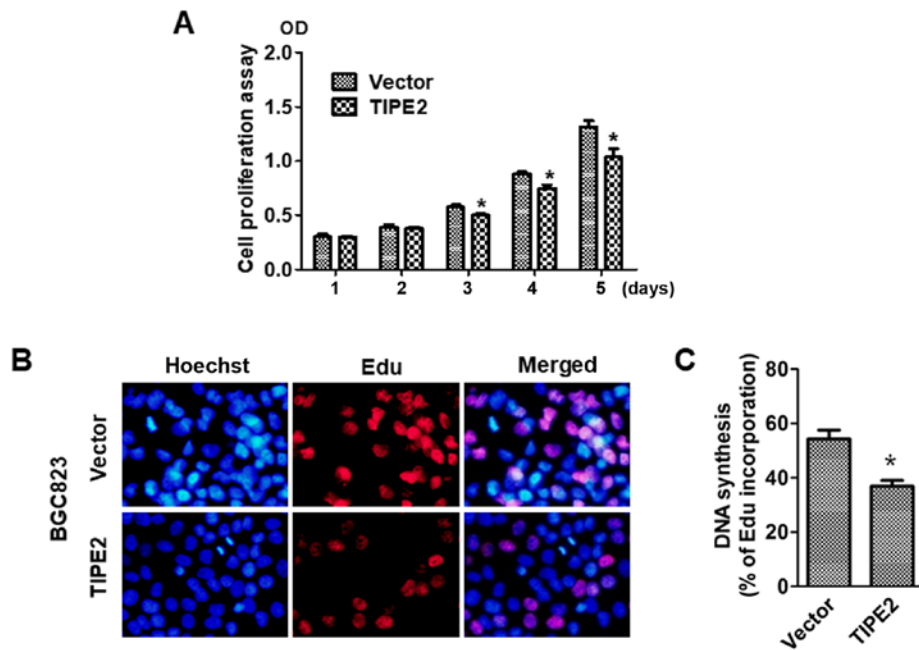
Figure 3. TIPE2 inhibits the proliferation of GC cells. (A) BGC823/Vector and BGC823/TIPE2 cells were evaluated at 1, 2, 3, 4 and 5-day time-points by CCK-8 assay. (B) GC cell lines were stained with Edu dye for 12 h and then observed with fluorescence microscope. (C) The percentage of cells that incorporated EdU. *P<0.05 vs. the vector group.
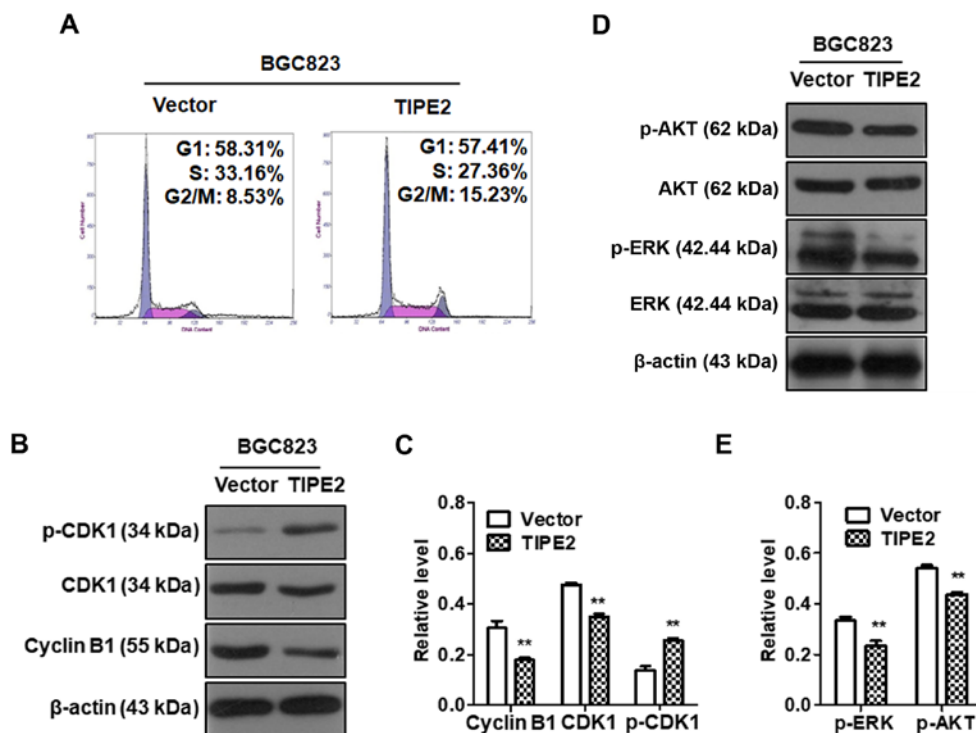

Figure 4. TIPE2 induces G_2/M phase cell cycle arrest. BGC-823/Vector and BGC-823/TIPE2 cells were serum-starved for 12 h and then cultured for another 24 h. The cell cycle distribution was detected by (A) flow cytometry. The cell-cycle related proteins (B) and the PI3K/AKT signaling pathway related proteins (D) were detected by western blotting. The expression of each index was normalized to the expression level of β-actin (C and E). **P<0.01 vs. the vector group.

cells were detected by western blot analysis. As displayed in Fig. 6B, TIPE2 overexpression clearly upregulated cleaved caspase-9, cleaved caspase-3 and cleaved PARP, as well as downregulated Bcl-2 in BGC823 cells. These results revealed that TIPE2 promoted the apoptosis of GC cells, possibly via activating the intrinsic apoptotic pathway.

To confirm whether TIPE2 affected the exogenous apoptosis pathway, we detected the activity of caspase-3, caspase-8 and caspase-9 in TIPE2 transfected and vector-transfected BGC823 cells. As displayed in Fig. 6C, the activity of caspase-3 and caspase-9 increased after TIPE2 overexpression, which was consistent with previous western blotting results.
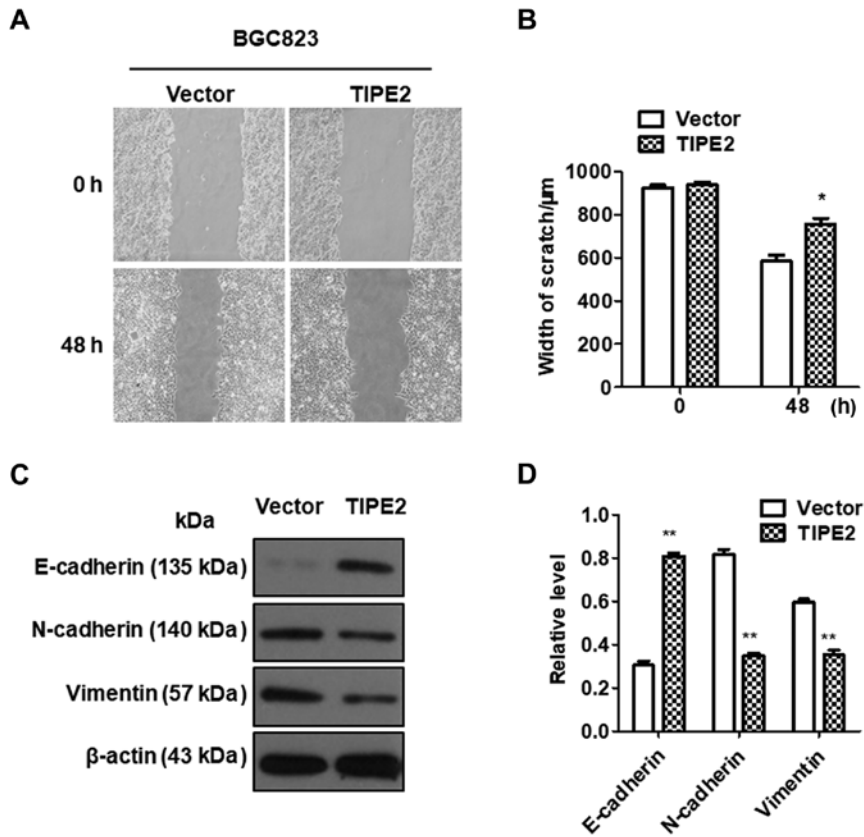
Figure 5. TIPE2 inhibits the migration of GC cells. BGC-823/Vector and BGC-823/TIPE2 cell monolayers were scratched with a white pipette tip. Cells were imaged at 0 and 48 h after wounding. (A) Representative images of wound healing are shown and (B) the gap distance was calculated using ImageJ software. (C) Expression changes of EMT-related factors were assessed via western blotting, and (D) the expression of each index was normalized to the level of β-actin. *P<0.05, **P<0.01 vs. the control vector group.
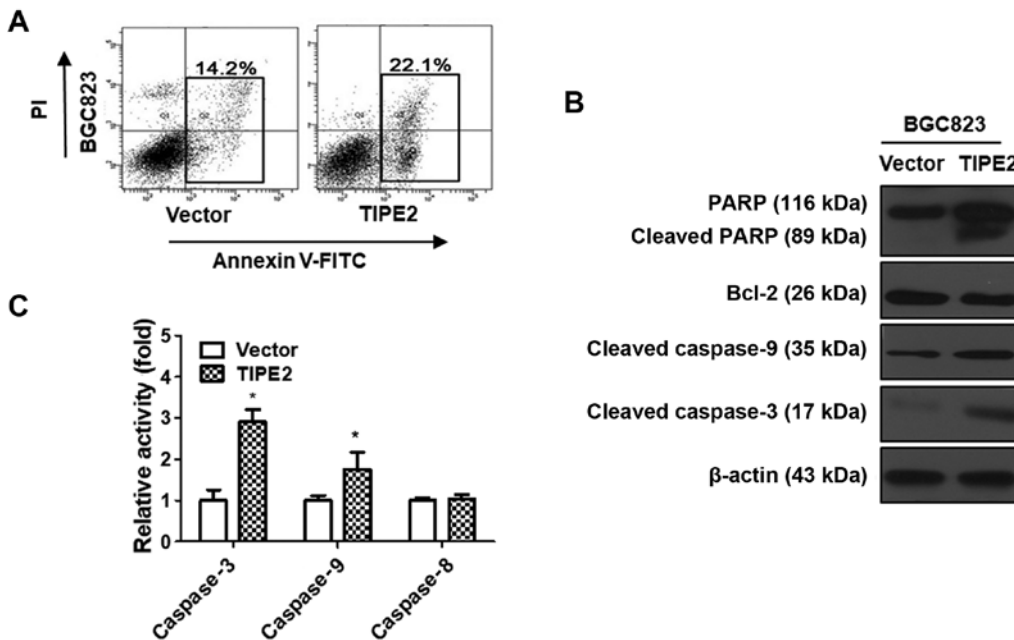

Figure 6. TIPE2 promotes GC cell apoptosis. BGC823 human GC cells were transiently transfected with GV218 or GV218-TIPE2 plasmids. (A) At 48 h after treatment, the cells were harvested, stained with PI and FITC-conjugated with Annexin V, and then analyzed by flow cytometry. (B) Apoptosis-related proteins were analyzed by western blotting and (C) the activity of caspases was detected using a commercial kit. *P<0.05 vs. the control vector group.

However, there was no difference in the activity of caspase-8 between TIPE2 transfected and vector transfected BGC823 cells. These results indicated that TIPE2 induced apoptosis through the endogenous apoptosis pathway.
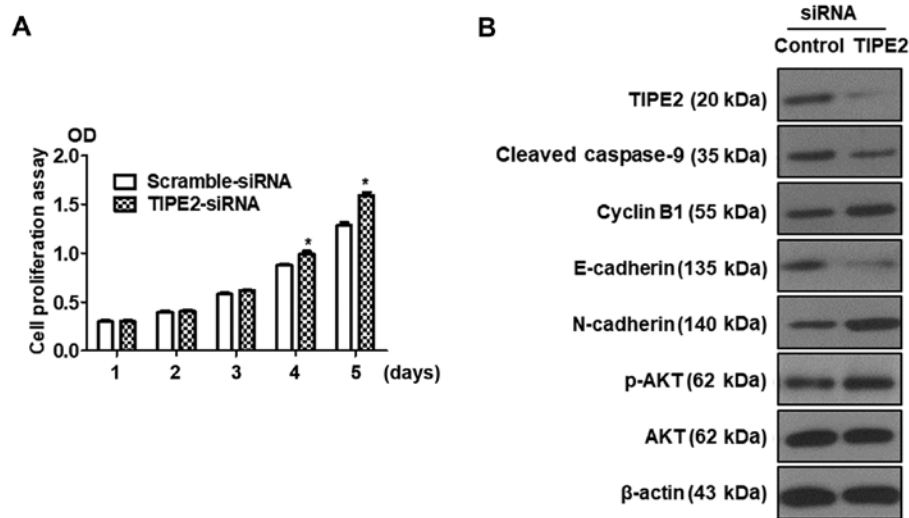
Figure 7. Silencing of TIPE2 promotes GC cell proliferation. (A) BGC823 cells were transfected with scramble siRNA or TIPE2-siRNA and evaluated at 1, 2, 3, 4 and 5-day time-points by CCK-8 assay, and (B) the related proteins were detected by western blotting after TIPE2 silencing. *$P<0.05$ vs. the control vector group.
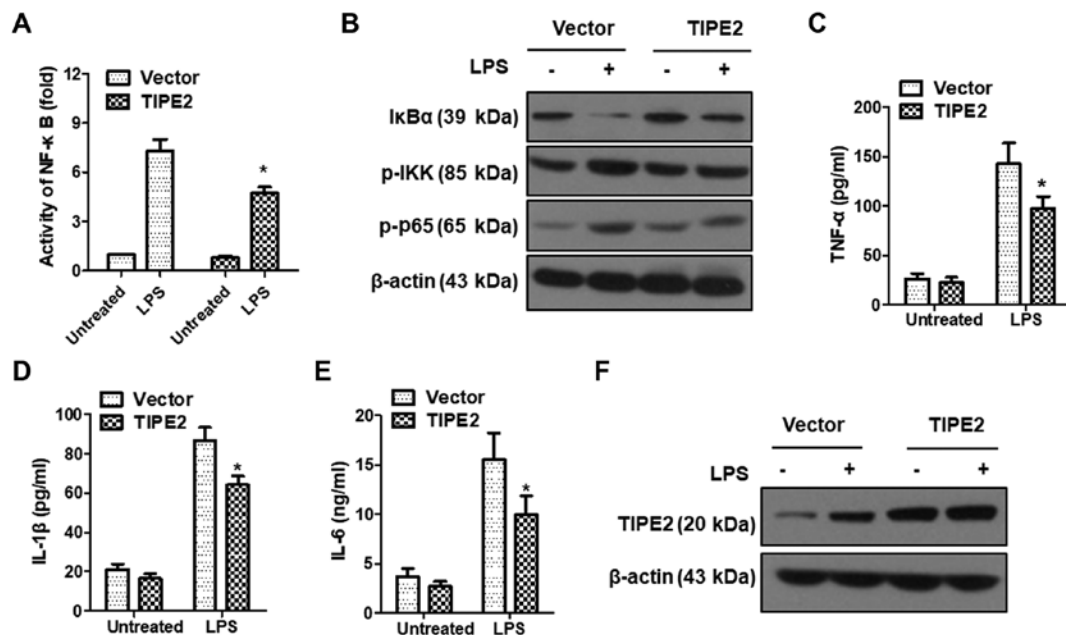

Figure 8. TIPE2 inhibits LPS-induced inflammation. (A) The NF-κB reporter gene plasmid and the *Renilla* plasmid were co-transfected into SGC7901/vector and SGC7901/TIPE2 cells for 24 h. Cells were treated with 20 ng/ml LPS for 12 h, and the relative transcriptional activity of NF-κB was then analyzed using a Dual-Luciferase reporter gene system. (B) SGC7901/vector and SGC7901/TIPE2 cells were stimulated with or without 20 ng/ml LPS for 30 min, and the expression of IκBα, p-IKK and p-p65 was detected by western blotting. (C-E) GC cell lines were stimulated with 20 ng/ml LPS for 24 h and the expression of various inflammatory factors was analyzed using an ELISA kit, and (F) the expression of TIPE2 was detected by western blotting. *$P<0.05$ vs. the control vector group.

Silencing of TIPE2 promotes GC cell proliferation and reverses the expression of related proteins compared with TIPE2 overexpression. Previous results revealed that TIPE2 inhibited the proliferation of BGC823 cells. Silencing of TIPE2 was performed to further confirm the effect of TIPE2 on proliferation. BGC823 cells were transfected with scramble siRNA or TIPE2-siRNA, and the viability of BGC823 cells was assessed at different time-points (days 1-5) by CCK-8 assay. As displayed in Fig. 7A, silencing of TIPE2 promoted BGC-823 tumor cell growth *in vitro* on days 4 and 5. In addition, we

detected the expression of related proteins by western blotting. As depicted in Fig. 7B, the expression of TIPE2 was shut down following transfection with TIPE2-siRNA, whereas the expression of p-AKT, N-cadherin and cyclin B1 was upregulated and the expression of E-cadherin and cleaved-caspase-9 was downregulated. These results were contrary to the results obtained with TIPE2 overexpression. The aforementioned results indicated that TIPE2 affected the function of GC cells not only in proliferation but also in apoptosis, the cell cycle and migration.

TIPE2 inhibits LPS-induced inflammation. LPS can activate NF-κB signaling by initiating an intracellular signaling cascade through the TLR4 pathway (20,21). By controlling the expression of inflammation-related genes, the activation of NF-κB plays a crucial role in enhancing the cellular inflammatory response (21). To verify the role of TIPE2 in LPS-induced inflammatory responses, we examined the effect of TIPE2 on NF-κB transcription activity in SGC7901 cells using a Dual-Luciferase Reporter Gene System (Promega). The results revealed that NF-κB activity was significantly enhanced following LPS induction, however the NF-κB activity increase in the TIPE2-overexpression group was significantly lower than that observed in the vector control group (Fig. 8A). Activation of NF-κB occurs when it is isolated from IκBα, and IκBα degrades after being phosphorylated. We further detected the expression of IκBα, p-IKK and p-p65 after LPS induction in SGC7901/vector and SGC7901/TIPE2 cells by western blotting. As displayed in Fig. 8B, the expression of p-IKK and p-p65 increased following LPS induction, but this was attenuated by TIPE2. The activation of NF-κB induced a large number of inflammatory factors such as IL-1β, IL-6 and TNF-α. To determine whether TIPE2 could inhibit the NF-κB signaling pathway, the levels of IL-1β, IL-6 and TNF-α were detected by ELISA after LPS-stimulation in the SGC7901/vector and SGC7901/TIPE2 groups. The results revealed that TIPE2 overexpression could inhibit LPS-induced expression of the inflammatory cytokines IL-1β, IL-6 and TNF-α (Fig. 8C-E). These results indicated that TIPE2 could inhibit LPS-induced inflammation by suppressing the NF-κB signaling pathway. Notably, LPS could upregulate the expression of TIPE2 in SGC7901/vector cells, but not in SGC7901/TIPE2 cells (Fig. 8F), which may be caused by the feedback of LPS-induced inflammation.

Discussion

The causes of GC are complex and only partially understood. Thus, many treatments indicated for GC are controversial. Certain clinical studies have observed that, during the development of GC, the expression profiles of specific biomolecules change. Such changes in expression may serve a key role in tumor progression, including the processes of cell proliferation (6,10,18,22,23), motility (24), adhesion (25), apoptosis and tissue inflammation. As an inflammatory inhibitor, TIPE2 not only induces cell death, but also inhibits Ras-induced tumor formation, providing a molecular bridge from inflammation to cancer. Research has revealed that TIPE2 is an important negative regulator of inflammation and carcinogenesis (26). Studies have revealed that TIPE2 also plays an important role in non-immune cells, including lung, stomach and liver cells (22,27). Compared with healthy individuals, it was revealed TIPE2 expression was significantly reduced in PBMCs from patients with chronic hepatitis B, chronic hepatitis C and systemic lupus erythematosus (14,15,27).

In the present study, we proposed a model to describe the function of TIPE2 in carcinogenesis. In gastric epithelium, inflammation induced by stimulatory reagents such as LPS (or pathogens such *Helicobacter pylori*) leads to increased cell apoptosis, and TIPE2 is necessary for this process. This could be a mechanism to eliminate cells that have been exposed to excessive free radicals generated by inflammation, and therefore to prevent the damaged cells from surviving and proliferating. Upon the reduction of TIPE2 expression, however, this process is inhibited and damaged cells have a better chance of survival and proliferation, thereby accumulating genomic mutations and eventually leading to carcinogenesis.

According to our clinical and biochemical data, the expression of TIPE2 in GC tissues was reduced or absent, and may be related to the occurrence and development of GC. TIPE2 inhibited the proliferation of GC cells by inhibiting p-AKT and p-ERK, thus inhibiting the PI3K-AKT and Ras-Raf-MEK-ERK1/2 signaling pathways. In addition, TIPE2 induced G_2/M-phase arrest by downregulating the expression of CDK1 and cyclin B1, while upregulating the expression of p-CDK1. TIPE2 inhibited the expression of Bcl-2 and increased the levels of cleaved-caspase-9 and cleaved-caspase-3, which promote endogenous apoptosis. Furthermore, TIPE2 inhibited the activation of NF-κB induced by LPS, as well as the expression of IL-1β, IL-6 and TNF-α, reducing LPS-induced cell proliferation.

The invasion and metastasis of tumors as the leading cause of death in cancer increases not only the suffering of patients, but also the difficulty of clinical treatment. EMT is an effective way for epithelial cells to acquire migratory capacity (18,19), it has become an important pathway for invasion and metastasis of epithelial cell carcinoma. Various studies have shown that the development of EMT is accompanied with changes in markers, including E-cadherin, N-cadherin and vimentin. In the present study, our results revealed that TIPE2 significantly inhibited the migration of GC cells accompanied with E-cadherin upregulation and N-cadherin and vimentin downregulation, thus indicating a new molecular mechanism by which TIPE2 regulated cell migration in gastric cells.

In conclusion, we presented TIPE2 as a potential therapeutic target for GC, and our results revealed that it functioned by reducing the migration and proliferation of GC cells.

Availability of data and materials

The datasets used during the present study are available from the corresponding author upon reasonable request.

Authors' contributions

ZQ, GZ and ZL researched idea and study design. ZL, WL, CX and YF performed data collection. ZQ, GZ, ZL and CX analyzed and interpreted data. All authors read and approved the manuscript and agree to be accountable for all aspects of the research in ensuring that the accuracy or integrity of any part of the work are appropriately investigated and resolved.

Ethics approval and consent to participate

Written informed consent for the study was provided by all participants. The study was approved by the Medical Ethics Committee of the Zhongshan Hospital of Xiamen University.

Patient consent for publication

Not applicable.

Competing interests

The authors declare that they have no competing interests.

References

1. Jemal A, Bray F, Center MM, Ferlay J, Ward E and Forman D: Global cancer statistics. CA: Cancer J Clin 61: 69-90, 2011.
2. Fang JY, Cheng ZH, Chen YX, Lu R, Yang L, Zhu HY and Lu LG: Expression of Dnmt1, demethylase, MeCP2 and methylation of tumor-related genes in human GC. World J Gastroenterol 10: 3394-3398, 2004.
3. Chen CN, Lin JJ, Chen JJ, Lee PH, Yang CY, Kuo ML, Chang KJ and Hsieh FJ: Gene expression profile predicts patient survival of GC after surgical resection. J Am Soc Clin Oncol 23: 7286-7295, 2005.
4. Nathan C and Ding A: Nonresolving inflammation. Cell 140: 871-882, 2010.
5. Sun HH, Gong S, Carmody RJ, Hilliard A, Li L, Sun J, Kong L, Xu L, Hilliard B, Hu S, *et al*: TIPE2, a negative regulator of innate and adaptive immunity that maintains immune homeostasis. Cell 133: 415-426, 2008.
6. Wang K, Ren Y, Liu Y, Zhang J and He JJ: Tumor necrosis factor (TNF)-alpha-induced protein 8-like-2 (TIPE2) inhibits proliferation and tumorigenesis in breast cancer cells. Oncol Res 25: 55-63, 2017.
7. Zhang X, Wang J, Fan C, Li H, Sun H, Gong S, Chen YH and Shi Y: Crystal structure of TIPE2 provides insights into immune homeostasis. Nat Struct Mol Biol 16: 89-90, 2009.
8. Xi W, Hu Y, Liu Y, Zhang J, Wang L, Lou Y, Qu Z, Cui J, Zhang G, Liang X, *et al*: Roles of TIPE2 in hepatitis B virus-induced hepatic inflammation in humans and mice. Mol Immunol 48: 1203-1208, 2011.
9. Zhang L, Shi Y, Wang Y, Zhu F, Wang Q, Ma C, Chen YH and Zhang L: The unique expression profile of human TIPE2 suggests new functions beyond its role in immune regulation. Mol Immunol 48: 1209-1215, 2011.
10. Fayngerts SA, Wang ZJ, Zamani A, Sun H, Boggs AE, Porturas TP, Xie W, Lin M, Cathopoulis T, Goldsmith JR, *et al*: Direction of leukocyte polarization and migration by the phosphoinositide-transfer protein TIPE2. Nat Immunol 18: 1353-1360, 2017.
11. Sun H, Zhuang G, Chai L, Wang Z, Johnson D, Ma Y and Chen YH: TIPE2 controls innate immunity to RNA by targeting the phosphatidylinositol 3-kinase-Rac pathway. J Immunol 189: 2768-2773, 2012.
12. Zhu Y, Tao M, Wu J, Meng Y, Xu C, Tian Y, Zhou X, Xiang J, Zhang H and Xie Y: Adenovirus-directed expression of TIPE2 suppresses GC growth via induction of apoptosis and inhibition of AKT and ERK1/2 signaling. Cancer Gene Ther 23: 98-106, 2016.
13. Zhao Q, Zhao M, Dong T, Zhou C, Peng Y, Zhou X, Fan B, Ma W, Han M and Liu S: Tumor necrosis factor-α-induced protein-8 like-2 (TIPE2) upregulates p27 to decrease gastic cancer cell proliferation.. J Cell Biochem 116: 1121-1129, 2015.
14. Cao XL, Zhang L, Shi YY, Sun Y, Dai S, Guo C, Zhu F, Wang Q, Wang J, Wang X, *et al*: Human tumor necrosis factor (TNF)-alpha-induced protein 8-like 2 suppresses hepatocellular carcinoma metastasis through inhibiting Rac1. Mol Cancer 12: 149, 2013.
15. Li XM, Su JR, Yan SP, Cheng ZL, Yang TT and Zhu Q: A novel inflammatory regulator TIPE2 inhibits TLR4-mediated development of colon cancer via caspase-8. Cancer Biomarkers 14: 233-240, 2014.
16. Ruan H, Zhan YY, Hou J, Xu B, Chen B, Tian Y, Wu D, Zhao Y, Zhang Y, Chen X, *et al*: Berberine binds RXRα to suppress β-catenin signaling in colon cancer cells. Oncogene 36, 6906-6918, 2017.
17. He K, Chen D, Ruan H, Li X, Tong J, Xu X, Zhang L and Yu J: *BRAF V600E*-dependent Mcl-1 stabilization leads to everolimus resistance in colon cancer cells. Oncotarget 7: 47699-47710, 2016.
18. Yao Y, Wang ZC, Liu JX, Ma J, Chen CL, Deng YK, Liao B, Wang N, Wang H, Ning Q, *et al*: Increased expression of TIPE2 in alternatively activated macrophages is associated with eosinophilic inflammation and disease severity in chronic rhinosinusitis with nasal polyps. Int Forum Allergy Rhinol 7: 963-972, 2017.
19. Sun Y, Wang X, Li Y, Sun H, Wan L, Wang X, Zhang L, Fang Z and Wei Z: The decreased expression of TIPE2 protein in the decidua of patients with missed abortion and possible significance. Reprod Biol Endocrinol 15: 68, 2017.
20. Li X, Zhang Y, Li F, Zhu X and Huang L: Negative immune regulatory molecule tipe2 for treating sle mice through regulating macrophage subtype. Chongqing Med 2017.
21. Zhang Y, Mei S, Zhou Y, Yang D, Pan T, Chen Z and Wang Q: TIPE2 negatively regulates mycoplasma pneumonia-triggered immune response via MAPK signaling pathway. Sci Rep 7: 13319, 2017.
22. Liu RL, Fan TT, Geng WW, Chen YHH, Ruan QG and Zhang C: Negative immune regulator TIPE2 promotes M2 macrophage differentiation through the activation of PI3K-AKT signaling pathway. PLoS One 12, e0170666, 2017.
23. Shi-Bai Z, Rui-Min L, Ying-Chuan S, Jie Z, Chao J, Can-Hua Y, Xi C and Wen-Wei Q: TIPE2 expression is increased in peripheral blood mononuclear cells from patients with rheumatoid arthritis. Oncotarget 8: 87472-87479, 2017.
24. Jiang JS, Wang SS, Fang J, Xu Y, Tong L, Ye X and Zhou W: Stable silencing of TIPE2 reduced the Poly I:C-induced apoptosis in THP-1 cells. Mol Med Rep 16: 6313-6319, 2017.
25. Zhang Z, Liu L, Cao S, Zhu Y and Mei Q: Gene delivery of TIPE2 inhibits breast cancer development and metastasis via CD8+ T and NK cell-mediated antitumor responses. Mol Immunol 85: 230-237, 2017.
26. Zhang G, Zhang W, Lou Y, Xi W, Cui J, Geng M, Zhu F, Chen YH and Liu S: TIPE2 deficiency accelerates neointima formation by downregulating smooth muscle cell differentiation. Cell Cycle 12: 501-510, 2013.
27. Kong L, Liu K, Zhang YZ, Jin M, Wu BR, Wang WZ, Li W, Nan YM and Chen YH: Downregulation of TIPE2 mRNA expression in peripheral blood mononuclear cells from patients with chronic hepatitis C. Hepato Int 7: 844-849, 2013.